C.Y. Wu[1], W.Q. Ling[2], Y.C. Yao[2], M. Guo[2*], N. Nuraje[3]

[1]College of Forestry, Tarim University, A'ler, Xinjinag, China;
[2]College of Chemistry and Materials Engineering, Zhejiang Agriculture & Forestry University, Hangzhou, Zhejiang, China;
[3]School of Engineering & Digital Science, Nazarbayev University, Nur-Sultan, Kazakhstan
*(*Corresponding author's e-mail: guoming@zafu.edu.cn)*

Three-Dimensional Fingerprint Spectroscopy Study on the Biopolymer System of Polyphenol Oxidase Binding with Cumalic Acid

The protection of Cumalic acid (CA), antioxidant, in the biochemical process in nature has aroused great interest. Polyphenol oxidase (PPO), an enzyme, plays a vital function in aging and browning of plants, such as vegetables, fruits, and mushrooms. The interaction of CA and PPO reveals the important information in metabolism and aging. Thus, the molecular mechanism of CA binding with polyphenol oxidase (PPO) was explored by combining spectroscopic methods with molecular modeling. A three-dimensional fingerprint of the CA-PPO complex was built for the first time to characterize the biopolymer interaction between CA and PPO. Application of the spectroscopic methods indicated that CA effectively quenched the intrinsic fluorescence of PPO. The enthalpy change ($\Delta H°$) and entropy change ($\Delta S°$) suggested that the CA-PPO complex was predominantly stabilized by hydrophobic interactions CA and PPO. Building the λ-UV-F fingerprint of CA-PPO made it possible to demonstrate the three-dimensional interactions between CA and PPO. Subsequently, molecular modeling demonstrated that CA was primarily bound to PPO by hydrophobic interactions and hydrogen bonds located at amino acid residues Ala202, His38, His54, and Ser206. The computational simulations were consistent with the spectral experiments demonstrating confidence in the three-dimensional model determined of the CA-PPO interaction.

Keywords: biopolymer, Cu-containing enzyme, coumaric acid, polyphenol oxidase, antioxidant, α-pyrone-5-carboxylic acid, spectroscopy, tyrosinase, molecular modeling.

Introduction

Polyphenol oxidase (PPO) is a multifunctional Cu-containing enzyme, which is also called tyrosinase and is found widely in living organisms, such as vegetables, fruits, and mushrooms [1, 2]. It is a paramount substance in the process of browning of fruits after contact with the oxygen in the air which occurs after damaged or long-term storage [3, 4]. The enzyme PPO is also involved in the production of melanin [5]. Specifically, PPO is involved in the formation of the melanin shield protecting plants from external stress.

The biochemical properties of phenolic resins have been extensively studied. They are reported to have antioxidants, anti-carcinogenic and other properties [6]. Due to the various pharmacological properties, antioxidants have been of great interest in recent years. The main mechanism proposed may play a protective role through the transfer of H atoms, single electron transfer, and metal chelation [7]. Cumalic acid (CA), also known as α-pyrone-5-carboxylic acid, is such an antioxidant (Figure 1). This antioxidant, CA, is the main active component of mature spores of tomato and lygodium japonicum plants [8]. It is also a potential candidate in the field of antioxidant, antibacterial and antiviral research [9]. According to the studies, both CA and PPO consist in the same plants and have effects on the metabolism of plants [10, 11]. Recently, several studies have been published related to molecular modeling studies of PPO [12–14]. However, research about interaction mechanism between CA and PPO has not yet been conducted.
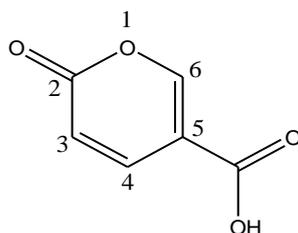
Figure 1. The structure of Cumalic acid

Rosario Goyeneche, Yue-Xiu Si, Mareike E. Dirks-Hofmeister, and many other professors have reported that PPO is associated with the active ingredient in plant tissues [15–17]. At present, some researchers mostly pay attention to the active molecule interactions with enzymes on the binding reaction between animal's protease and drug molecules [18–20], while others are focused on the reactive molecules inhibited enzyme activity [21, 22]. There are a plethora of investigations on the enzyme interactions and enzyme inhibitions in animals and humans because enzymes are one of the most important targets for drugs to exert effects on the body. However, there are a few studies on the interaction between plant enzymes and active plant components. Thus, it will be important to understand in more detail how plant processes such as aging or browning may affect enzyme activities.

Many research literature show that fluorescence and UV-*vis* absorption spectroscopy techniques are powerful tools for studying important data of complexes. The values of wavelength (λ), fluorescence intensity (F), and ultraviolet absorption (A) can be extracted from the spectral experiment, which helps to draw a three-dimensional fingerprint of λ ~ F~A and analyze the fingerprint peaks to obtain the interaction characteristics of small molecules and enzymes. Therefore, the construction of traditional Chinese medicine fingerprint can primarily reflect the species and quantity of chemical composition in traditional Chinese medicine, and make an integral description and evaluation of the quality of medicine [23]. Based on the construction principle of traditional Chinese medicine fingerprint and spectrum experiment skills, we get and extract the absorption spectrum and emission spectrum data of CA binding with PPO.

In this work, fluorescence and UV-*vis* absorption spectroscopy are measured to detect the interaction mechanism between CA and PPO. The *λ-UV-F* fingerprint is built to analyze characteristic fingerprint peaks in the CA-PPO fingerprint chromatogram, which aims to explore and reveal the binding between CA and PPO. The molecular modeling is also constructed to explain and support data from the spectral experiment. We believe these findings will be useful for pharmaceutical research, especially for the synthesis and design of CA derivatives with enhanced activity.

Experimental

Reagents and Materials

1.0×10^{-6} mol·L^{-1} of PPO (3130 units/mg) (Sigma Chemical USA) in phosphate-buffered saline (PBS, pH 6.5) at CA (≥97 %) (Energy Chemical Shanghai), and 1.0×10^{-4} mol·L^{-1} in ethanol were prepared separately. Ultrapure water was used to prepare for the above solutions. All chemicals are of analytical grade.

Spectroscopic techniques which were used to measure fluoresce and absorption include the F-7000 spectrofluorophotometer (Hitachi, Japan) and UV-2450 UV-vis spectrometer (Shimadzu, Japan). A BS224 Selectronic analytic weighing scale (Sartorius, China) was used to obtain the precise amount of the samples for experiment.

Experimental procedure for spectroscopic measurement

The absorption spectra of PPO in the presence of CA ranging from 0 to 5.6×10^{-6} mol·L^{-1} were measured in the range of 200–800 nm at room temperature. The conditions for fluorescence measurement were set at 291 K, 300 K, and 308 K. The emission spectra were recorded in the wavelength range of 250–500 nm upon excitation at 282 nm with a scanning speed of 1200 nm/min. The widths of both the excitation slit and emission slit were set to 5 nm. The fluorescence emission spectra of PPO were recorded in the absence and presence of increasing concentrations of CA, corresponding to 0×10^{-6}, 0.4×10^{-6}, 0.8×10^{-6}, 1.0×10^{-6}, 1.8×10^{-6}, 2.4×10^{-6}, 3.2×10^{-6}, 4.0×10^{-6}, 4.8×10^{-6}, 5.6×10^{-6} mol·L^{-1}. Subtract the appropriate blank corresponding to the buffer to correct the fluorescent background.

λ-UV-F fingerprint

The three-dimensional fingerprint of the CA-PPO complex was built using emission wavelength, intensity of fluorescence, and UV absorption values from the CA-PPO spectral experiments. The interaction characteristics of the CA-PPO system were obtained by analyzing the peak distributions of fingerprint spectrum.

Molecular modeling: blind docking simulation

PPO (tyrosinase) belongs to the oxidase superfamily protein [24, 25]. To understand the basic mechanism of PPO and CA interaction, in the experiment, the docking mode of CA was checked at the catalytic site of PPO. The binding site was fixed near the three fluorophores (Trp, Tyr, and Phe) under the guidance of a fluorescence experiment. The three-dimensional structure of PPO was obtained from the Protein Data Bank (PDB ID: 1WX2). The CA structure was built using ChemDraw Ultra 8.0 software. For the docking of CA with PPO, the required files for ligand (CA) were created through Gaussian. The following steps taken for

the docking process were: (1) conversion of the 2D structure to a 3D structure; (2) addition of hydrogen atoms; (3) calculation of charges, and (4) location of pockets. The PyMOL software package was used for the visualization of the docked conformations. Finally, all experimental data calculations from our work were performed on a Silicon Graphics Ocatane2 workstation.

Calculation equations

Dynamic quenching is the mechanism of fluorescence quenching. The calculation is disclosed as follows [26]:

$$\frac{F_0}{F} = 1 + K_{sv[Q]} = 1 + K_q\tau_{0[Q]}, \tag{1}$$

where K_q, K_{sv}, τ_0 and $[Q]$ — the quenching rate constant of the biomolecule, the dynamic quenching constant, the average lifetime of molecule without quencher and the concentration of quencher, respectively.

The K_{sv} and dynamic quenching parameters of CA and PPO can be obtained from the experimental data by using the calculated equation (1). For the fluorescence lifetime of the biopolymer is 10^{-8} s, the quenching constant K_q (L·mol^{-1}·s^{-1}) can be obtained from $K_q = K_{sv}/\tau_0$.

For static quenching interaction, experimental numerical calculation and determination can be performed according to formula (2) [27, 28]:

$$\lg\left[(F_0 - F)/F\right] = \lg K + n\lg[Q]. \tag{2}$$

Among them, F_0, F, and $[Q]$ are the same as defined in formula (1), K is the binding constant in CA and PPO, and n is the number of binding sites in each PPO molecule, and it can be determined by the slope and intercept of double logarithm regression curve of $\lg[(F_0-F)/F]$ *vs.* $\lg[Q]$ based on Equation (2) (Figure 4).

The thermodynamic parameters of CA-PPO are calculated by the van't Hoff equation:

$$\ln K = \frac{-\Delta H°}{RT} + \frac{\Delta S°}{R}, \tag{3}$$

$$\Delta G° = \Delta H° - T\Delta S°, \tag{4}$$

where R — the universal gas constant, K at temperature T; T — the Kelvin temperature (291 K, 300 K, and 308 K).

In this research work, we calculated the energy transfer efficiency E based on the Föster's non-radioactive energy transfer theory. For the distance r, we calculated the distance from the ligand to the protein tryptophan residue, and R_0 is the Föster critical distance, at which 50 % of the excitation energy is transferred to the receptor. It can be calculated by using formula (5):

$$E = 1 - \frac{F}{F_0} = \frac{R_0^6}{\left(R_0^6 + r^6\right)}, \tag{5}$$

$$R_0^6 = 8.8 \times 10^{-25} K^2 N^{-4} \varphi J \tag{6}$$

where $K^2 = 2/3$, $N = 1.336$, $\varphi = 0.118$, J — the overlap integral of the fluorescence emission spectrum of the donor and that of the absorption spectrum of the acceptor.

Therefore,

$$J = \int_0^\infty F(\lambda)\varepsilon(\lambda)\lambda^4 d\lambda \bigg/ \int_0^\infty F(\lambda)d\lambda \tag{7}$$

where $F(\lambda)$ — the fluorescence intensity of the fluorescent donor at wavelength λ, $\varepsilon(\lambda)$ — the molar absorptivity of the acceptor at wavelength λ.

Results and Discussion

UV and fluorescence spectra of PPO in the presence of CA

In the UV-Vis absorption spectrum of PPO (Figure 2A), we observed a double absorption peak, but the peaks that appeared earlier in the study are generally ignored. Therefore, the maximum absorption peak of PPO is between 300 nm and 350 nm, and a red shift occurs, indicating that the existing CA ring molecular structure makes the system's hydrophobicity lower. The preliminary results indicated the formation of CA-PPO complex. In addition, because PPO molecules contain tryptophan, tyrosine, and phenylalanine, they have endogenous fluorescence (between 300 and 500 nm). When the excitation wavelength (λ_{ex}) is 282 nm, the maximum emission wavelength of PPO is about 351 nm. At this time, the fluorescence of PPO mainly comes from tryptophan residues.

At different concentrations of CA (1 to 10 in Figure 2B), the shape of the fluorescence spectrum of PPO did not change. As the concentration of CA increases, the maximum fluorescence emission peak of PPO red-shifts at 349 nm, indicating that the microenvironment of tryptophan (TRP) residues is reduced in hydrophobicity [29]. The increase in CA concentration leads to the contraction of the peptide chain near the binding site, and the hydrophobicity of the surrounding environment increases. The experimental results of different changes in the fluorescence spectrum and ultraviolet-visible spectrum show that there is an interaction between CA and PPO. Figure 2 shows that CA has no peak at the peak position of PPO and has no influence on the CA-PPO system.
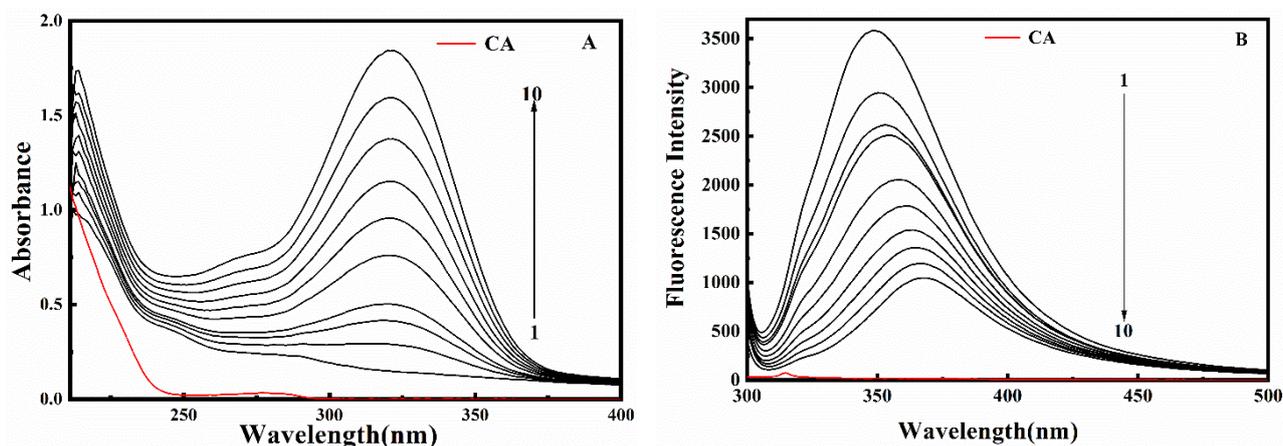
Figure 2. UV absorption spectra (*A*) and fluorescence spectra (*B*) of PPO in PBS solution in presence of various CA concentrations corresponding to 0×10^{-6}, 0.4×10^{-6}, 0.8×10^{-6}, 1.0×10^{-6}, 1.8×10^{-6}, 2.4×10^{-6}, 3.2×10^{-6}, 4.0×10^{-6}, 4.8×10^{-6}, 5.6×10^{-6} mol·L^{-1} from 1 to 10; pH = 6.5; $c_{(ppo)} = 1.0\times10^{-6}$ mol·L^{-1}

Quenching mechanism of PPO with CA

It can be seen from Figure 2B that as the concentration of CA increases, the fluorescence of tryptophan residues decreases, which can be explained why the compound is formed from CA and PPO. If the process of fluorescence quenching is dynamic quenching, then it can be described by an equation (1).
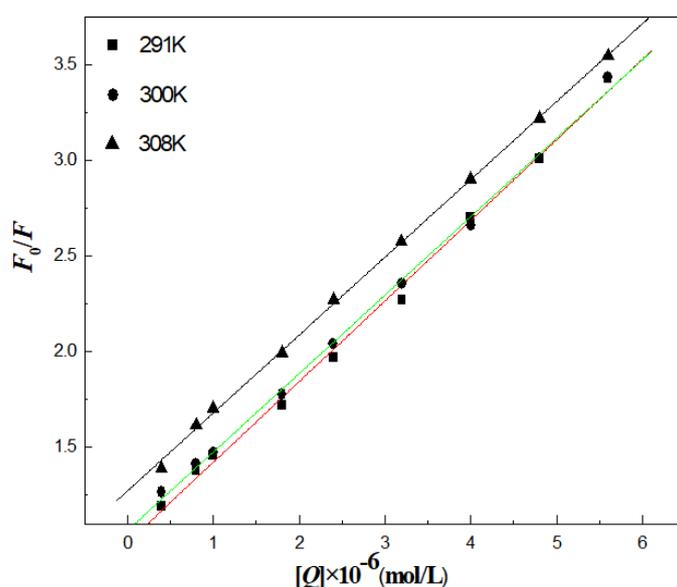
($\blacksquare$ — 291K; $\bullet$ — 300K; $\blacktriangle$ —308K). $c_{(ppo)} = 1.0\times10^{-6}$ mol·L^{-1}; pH = 6.5; $\lambda_{ex} = 282$ nm

Figure 3. The Stern-Volmer plot of PPO quenched by CA

The parameters of the Stern-Volmer plots for the quenching of PPO by CA at 291 K, 300 K, and 308 K

System	T(K)	K_{sv}(L·mol^{-1})	K_q(L·(mol·s)$^{-1}$)	R	SD
	291	4.22×10^4	4.22×10^{12}	0.99812	0.05127
CA-PPO	300	4.18×10^4	4.18×10^{12}	0.99882	0.04029
	308	3.23×10^4	3.23×10^{12}	0.99958	0.01850

The experimental results in Figure 3 and Table 1 indicate that the quenching curves of CA and PPO are different at different experimental temperatures. The curve obtained at each experimental temperature shows a good linear relationship between F_0/F and Q (R_{291}, R_{300}, $R_{308} > 0.99$), which illustrates the uniformity of static quenching. In addition, because the rate constant of CA-induced PPO is much larger than the K_q value of the dispersion process 2.0×10^{10} L·(mol·s)$^{-1}$ [19], in this experiment, quenching was not initiated by dynamic quenching, but it was caused by static quenching. In this process, compounds are formed. All the above data and results confirm that quenching between substances was caused by static quenching.

Binding constant and binding sites of PPO with CA

The value of the static quenching interaction can be obtained from equation (2). The results are shown in Figure 4 and Table 2.
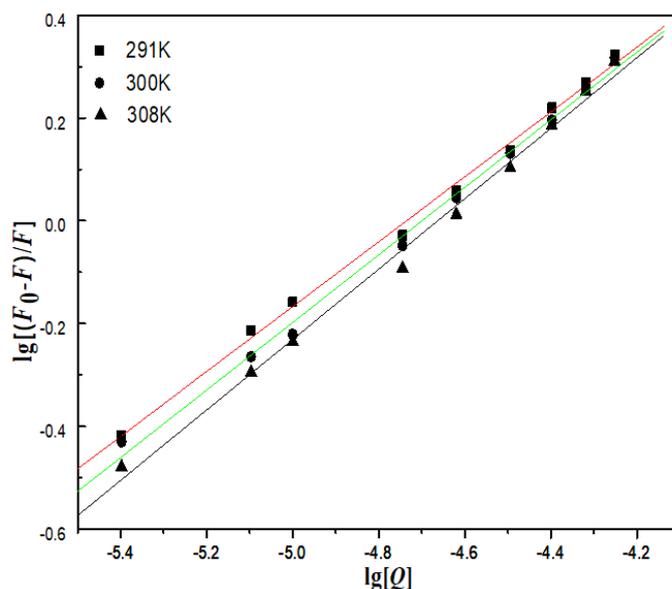
C(polyphenol oxidase) $= 1.0 \times 10^{-6}$ mol·L^{-1}; pH = 6.5; $\lambda_{ex} = 282$ nm

Figure 4. Plots of lg[$(F_0 – F)/F$] vs. lg[Q] for CA-PPO

The binding constants K, binding sites n and the thermodynamic parameters of CA-PPO system

System	T(K)	K(L·mol^{-1})	n	R	$\Delta G°$(kJ·mol^{-1})	$\Delta H°$(kJ·mol^{-1})	$\Delta S°$(J·(mol·K)$^{-1}$)
	291	2.45×10^4	0.95	0.9983	-26.08		
CA-PPO	300	1.86×10^4	0.92	0.9978	-27.21	28.66	188.09
	308	1.58×10^3	0.69	0.9970	-29.27		

The n value of CA-PPO complex in Table 2 is approximately equal to 1, indicating that there is one binding site in PPO for CA during their interactions. In Table 2, the binding constants are shown as a straight line at the three test temperatures. The higher the substance concentration, the lower the K value, shows that the test temperature has an influence on it.

Thermodynamic parameters and binding Forces

The sign and size of the parameters related to the drug-protein interaction process (such as ($\Delta H°$) and ($\Delta S°$)) can be used as some potential tools for deciphering the activation binding force [30, 31]. The calculated thermodynamic parameters collected in Table 2 show that $\Delta H°>0$，$\Delta S°>0$ (According to the relative magnitudes of thermodynamic enthalpy change $\Delta H°$ and entropy change $\Delta S°$ before and after the reaction, the main force types between small molecules and proteins can be judged [32]: when $\Delta S°>0$, it may be hydrophobic and electrostatic forces. $\Delta S°<0$ may be hydrogen bonding and van der Waals force, $\Delta H°>0$, $\Delta S°>0$ is a typical hydrophobic force; $\Delta H°<0$, $\Delta S°<0$ is mainly hydrogen bonding and van der Waals force), which manifest that the predominance of hydrophobic forces as the responsible factor for CA-PPO binding. This inference is well supported from blind docking simulation result which shows a hydrophobic force between the two molecules.

Energy transfer from PPO to CA

From Equation (5), Equation (6) and Equation (7), the following data was obtained: $E = 0.708$, $J = 1.11\times10^{-14}$ (cm^3·L)·mol^{-1}, $R_0 = 2.46$ nm, and $r = 2.13$ nm for the CA-PPO system. The donor-acceptor distances (*r*) of above CA-PPO system was less than 7 nm [33, 34], suggesting that the energy transfer from PPO to CA occurred with high probability. The distance values here are a theoretical value [35].

Three-dimensional fingerprint study

The three-dimensional spectrum of fluorescence intensity-absorbance-wavelength of CA-PPO system is preliminary constructed based on fingerprint construction technology (Figure 5). *λ-UV-F* fingerprint showed 4 characteristic peaks (Table 3).
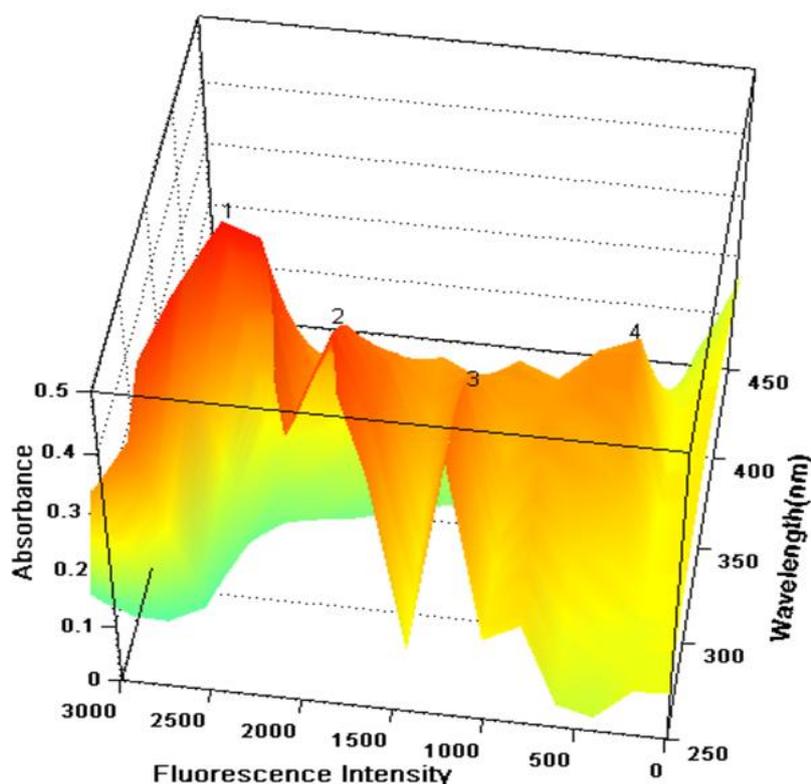
Figure 5. The three-dimensional spectra of wavelength-fluorescence intensity-absorbance ($C_{CA} : C_{PPO} = 1:1$)

Table 3

The data information of the CA-PPO three-dimensional fingerprint

Peak numbers	1	2	3	4
Absorbance(*A*)	0.164	0.298	0.372	0.1
Fluorescence intensity(*F*)	2511	2188	1288	2433
$F\times A$ (%)	4.12	6.52	4.79	2.43

The interaction mechanism between plant active ingredients CA and plant enzyme PPO is characterized by the fingerprint spectra. The fingerprint result is applied to reveal the dynamic change law of the PPO-CA system and lay a foundation for conducting an in-depth study of active ingredient CA binding with PPO in a different way. This experiment is based on the whole fingerprint to identify the authenticity of interaction. We select four characteristics of the spectrum and use the peak position and proportion of intensity as characteristic value to clearly express the specificity of fingerprint. The presence of many characteristic peaks in the three-dimensional fingerprint (Figure 5) proves that it has good stability and controllability. We think this method can provide a reference for establishing standard fingerprint spectra of the CA-PPO system.

Molecular docking simulation study

Based on the experimental target receptor calculation model Figure 6 illustrates the best energy ranking results.

(A)

(B)

(C)

Figure 6. Interaction mode (*A*) only residues around 20.0 Å of the CA (The residues of PPO are represented using blue ball model and the CA structure are represented using red ball model), hydrophobic surface map (B) and interaction mode (*C*) between CA and PPO are displayed (The CA structure are represented using green stick model, thereinto red sticks represented oxygen, the hydrogen bond between CA and PPO is represented using red dashed line)

Figure 6A presents the tryptophan residues Trp62, Trp184, and Trp213 within a 2 nm distance. The CA molecule, when brought into contact with PPO, was located close to the amino acid residues (Trp62, Trp184, Trp213, and Phe59) that have endogenous fluorescence. These experimental results effectively explain the

effective fluorescence quenching of PPO emission in the presence of CA. Spectrum experiment results showed that the microdomain of the PPO tryptophan residues and CA have obvious interactions with each other. The distance between PPO tryptophan (the donor) and CA (the acceptor) obtained from the fluorescence quenching experiment is nearly 2 nm. This distance measurement was corresponding to the combined distance measured by docking, which fully provides evidence that CA can quench the fluorescence spectra of PPO.

As shown in Figure 6B, the hydrophobic cavity in PPO has the function of containing active ingredients and an important position in various processes of CA. It can be seen from Figure 6C that the hydrogen-bond interaction occurred between oxygen atom on 2-bit =O and Ala202, between the oxygen atom on 5-bit formic =O and His54, between the oxygen atom on 5-bit formic -OH and His38, and between hydrogen atom and Ser206. CA rings were embedded in the bonded zone, PPO amino acids showed the stability of the CA-PPO system. Hydrogen bonding has the effect of reducing hydrophilicity and increasing hydrophobicity and can keep the CA-PPO system stable. Therefore, it can be concluded that hydrophobic forces and hydrogen bonding play a role between CA and PPO. Although there is little difference in the result between spectroscopic experiment and molecular modeling, the result of molecular modeling correlated well with the binding mode observed by the fluorescence quenching mechanism of PPO in presence of CA, *i.e.,* the hydrophobic interactions as the predominant interaction.
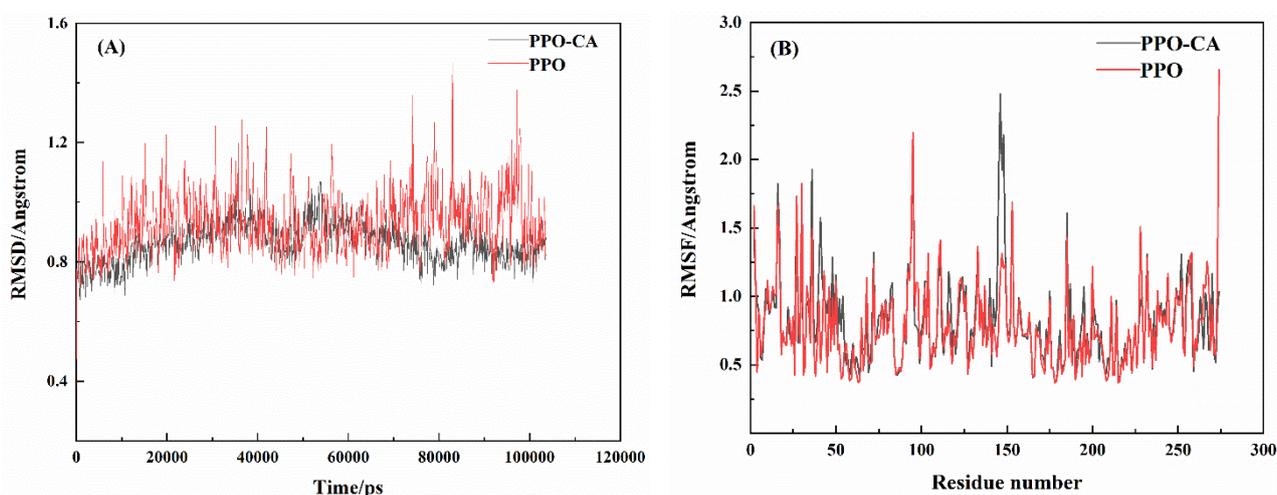
Figure 7. (*A*) Curves of RMSD values of PPO and PPO-CA over time;
(*B*) RMSF values and time of Cα carbon atoms in the skeletons of PPO and PPO-CA systems

The spatial conformation of the interaction between CA and PPO was studied by molecular dynamics simulation, and different parameters were calculated in vitro. RMSD (Figure 7A) demonstrates that within 90–110 ns, the fluctuation value of PPO-CA's RMSD is relatively low. The average RMSD value of PPO-CA is 0.863 A, and that of PPO is 0.927 A. It can be noticed that PPO-CA has a relatively rigid structure compared to PPO. CA has a significant effect on the conformation of PPO. The RMSF value reflects the fluctuation of amino acid residues in PPO relative to the average position and determines the flexibility of PPO in a given region of protein. The greater the RMSF value, the greater the fluctuation of amino acid residues. According to the RMSF (Figure 7B), the RMSF value fluctuates within the range of 0-3, indicating that the overall structure of PPO and PPO-CA is stable. The amino acid residue of PPO-CA is SER14, compared with that of CA-free PPO, ALA14 and ARG9 have large RMSF values, indicating that these parts are relatively flexible. Compared with the same parts of PPO residues, amino acid residues such as ALA40, LEU274, ALA41, ARG53 and ARG95 had lower RMSF values, and the amino acids in the active site were relatively stable and moved less, resulting in lower structural flexibility in this region. The results showed that PPO-CA was stable after equilibrium.

Conclusions

Based on the traditional drug-protein binding theory, this paper examined the interaction between CA and PPO from multiple perspectives. According to the fluorescence spectrum results, CA quenched the fluorescence of PPO by forming a PPO-CA complex, i.e., the static quenching, which is consistent with the hy-

potheses. CA can strongly bind to PPO. The increase in the temperature caused a decrease in the binding strength. According to the results of thermodynamic analysis, the binding force between CA and PPO is mainly hydrophobic interaction. The donor-acceptor distance (r) of the CA-PPO system was less than 7 nm, which indicates that the energy transfer from PPO to CA occurred. Three-dimensional spectrums (fluorescence intensity-absorbance-wavelength) of CA-PPO were preliminary constructed based on spectrum dates and the characteristic peaks of the interaction to verify the results ultimately.

Experimental results confirmed the interaction and micro binding domain between CA and PPO. Here it can be pointed out that the interaction was dominated by hydrophobic interaction and hydrogen bonding, which is consistent with the spectroscopy experiments.

The saturation of the enzyme PPO binding sites can be measured by the equilibrium experiment method, and it can help to analyze the binding mechanism. Important insights into the interaction of PPO with CA provided a useful guideline for further pharmacology research.

References

1   Siddiq, M., & Dolan, K.D. (2017). Characterization of polyphenol oxidase from blueberry (Vaccinium corymbosum L.). *Food Chem., 218*, 216–220. https://doi.org/10.1016/j.foodchem.2016.09.061

2   Anaya-Esparza, L.M., Velázquez-Estrada, R.M., Sayago-Ayerdi, S.G., Sánchez-Burgos, J.A., Ramírez-Mares, M.V., LourdesGarcía-Magaña, M., & Montalvo-González, E. (2017). Effect of thermosonication on polyphenol oxidase inactivation and quality parameters of soursop nectar. *LWT--Food Sci. Technol., 75*, 545–551. https://doi.org/10.1016/j.lwt.2016.10.002

3   Li, J., Wang, H., Yang, L., Mao, T., Xiong, J., He, S.L., & Liu, H. (2019). Inhibitory effect of tartary buckwheat seedling extracts and associated flavonoid compounds on the polyphenol oxidase activity in potatoes (*Solanum tuberosum* L.). *J. Integr. Agric., 18*(9), 2173–2182. https://doi.org/10.1016/S2095-3119(19)62692-4

4   Truong A,. N., Thor, Y., Harris, G. K., Simunovic, J., & Truong, V.D. (2019). Acid Inhibition on Polyphenol Oxidase and Peroxidase in Processing of Anthocyanin-Rich Juice and Co-product Recovery from Purple-Fleshed Sweetpotatoes: Sweetpotato juice. *J. Food Sci., 84*(7), 1730–1736. https://doi.org/10.1111/1750-3841.14664

5   Jiang, Y., Duan, X., Qu, H., & Zheng, S. (2016). Browning: Enzymatic Browning. Encycl. *Food Health*, 508–514. https://doi.org/10.1016/B978-0-12-384947-2.00090-8

6   Pollastro, F., Minassi, A., & Fresu, L.G. (2018). Cannabis Phenolics and their Bioactivities. *Curr. Med. Chem., 25*(10), 1160–1185. https://doi.org/10.2174/0929867324666170810164636

7   Zhaoming, Y., Yinzhao, Z., Yehui, D., Qinghua, C., & Fengna, L. (2020). Antioxidant mechanism of tea polyphenols and its impact on health benefits. *Animal Nutrition., 6*(2), 115–123. https://doi.org/10.1016/j.aninu.2020.01.001

8   Erdinc, C., Ekincialp, A., Gundogdu, M., Eser, F., & Sensoy, S. (2018). Bioactive components and antioxidant capacities of different miniature tomato cultivars grown by altered fertilizer applications. *J. Food Meas. Charact., 12*, 1519–1529. https://doi.org/10.1007/s11694-018-9767-7

9   Wen, R., Lv, H., Jiang, Y., & Peng, F.T. (2018). Anti-inflammatory isoflavones and isoflavanones from the roots of Pongamia pinnata (L.) Pierre. *Bioorg. Med. Chem. Lett., 28*(6), 1050–1055. https://doi.org/10.1016/j.bmcl.2018.02.026

10   Sukhonthara, S., Kaewka, K., & Theerakulkait, C. (2016). Inhibitory effect of rice bran extracts and its phenolic compounds on polyphenol oxidase activity and browning in potato and apple puree [J]. *Food Chem., 190*, 922–927. https://doi.org/10.1016/j.foodchem.2015.06.016

11   Guo, M., Zhao, X.X., Brodelius, P. E., Fang, L., Sun, Z.H., & Wang, R. (2020). The difference of Serum Protein Transport between Echinosides and Verbascoside. *Journal of the Chemical Society of Pakistan, 42*(3), 369–381. https://doi.org/10.52568/000651/jcsp/42.03.2020

12   Liu, F., Zhao, J.H., Wen, X., & Ni, Y.Y. (2015). Purification and structural analysis of membrane-bound polyphenol oxidase from Fuji apple. *Food Chem., 183*, 72–77. https://doi.org/10.1016/j.foodchem.2015.03.027

13   Zhou, Q.T., Guo, M., Ni, K.J., & Francesca, M.K. (2021).Construction of supramolecular laccase enzymes and understanding of catalytic dye degradation using multispectral and molecular docking approaches. *Reaction Chemistry & Engineering, 6*: 1940–1949. https://doi.org/10.1039/D1RE00111F

14   Brasil, E.M., Canavieira, L.M., Cardoso, É.T., Silva, E.O., Lameira, J., Nascimento, J., Eifler-Lima, V.L., Macchi, B.D., Sriram, D., Bernhardt, P.V., Silva, J.R., Williams, C.M., & Alves, C.N. (2017). Inhibition of tyrosinase by 4H chromene analogs: Synthesis, kinetic studies, and computational analysis. *Chemical Biology & Drug Design, 90*, 804–810. https://doi.org/10.1111/cbdd.13001

15 Guo, M., Lv, D., Shao, C Y, Kuang, Y, & Sun, Z.H. (2019). Analysis of the interaction mechanisms of polysaccharide homologs binding with serum albumin using capillary electrophoresis. *Journal of the Chemical Society of Pakistan, 41*(4), 640–649. https://doi.org/10.52568/000780/jcsp/41.04.2019

16 Guo, M., Wang, Y., Wang, X.M., Jiang, Y.K., & Zhang, Y. (2018). Molecular interaction mechanism of tyramine, phenethylamine binding with adrenergic receptor β2. *Journal of The Chemical Society of Pakistan, 40*(1), 145–157. https://inis.iaea.org/search/search.aspx?orig_q=RN:49051002

17 Yue, L., Lee, J., Lü, Z., Yang, J., Ye, Z., & Park, Y. (2017). Effect of Cd^{2+} on tyrosinase: Integration of inhibition kinetics with computational simulation. *International journal of biological macromolecules, 94 Pt B*, 836–844. https://doi.org/10.1016/j.ijbiomac.2016.09.001

18 Sukhonthara, S., Kaewka, K., & Theerakulkait, C. (2016). Inhibitory effect of rice bran extracts and its phenolic compounds on polyphenol oxidase activity and browning in potato and apple puree. *Food chemistry, 190*, 922–927. https://doi.org/10.1016/j.foodchem.2015.06.016

19 Agudelo, D., Bourassa, P., Bariyanga, J., & TajmirRiahi, H.A. (2018). Loading efficacy and binding analysis of retinoids with milk proteins: a short review. *Journal of Biomolecular Structure and Dynamics, 36*, 4246–4254. https://doi.org/10.1080/07391102.2017.1411833

20 Guo, M., Wang, X.M., Lu, X.W., Wang H.Z., & Brodelius, P.E. (2016). α-Mangostin extraction from the native mangosteen (*Garcinia mangostana* L.) and the binding mechanisms of α-mangostin to HSA or TRF. *PLOS one, 11*(9), 1–22. https://doi.org/10.1371/journal.pone.0161566

21 Nixha, A.R., Ergun, A., Gençer, N., Arslan, O., & Arslan, M. (2019). Development of carbazole-bearing pyridopyrimidine-substituted urea/thiourea as polyphenol oxidase inhibitors: synthesis, biochemistry, and theoretical studies. *Archives of Physiology and Biochemistry, 125*, 263–269. https://doi.org/10.1080/13813455.2018.1453523

22 Nguyen, K., Cuellar, C., Mavi, P.S., LeDuc, D., Bañuelos, G., & Sommerhalter, M. (2018). Two poplar hybrid clones differ in phenolic antioxidant levels and polyphenol oxidase activity in response to high salt and boron irrigation. *J. Agric. Food Chem., 66*(28), 7256–7264. https://doi.org/10.1080/13813455.2018.1453523

23 Shao, M., Li, X., Zheng, K., Jiang, M., Yan, C., & Li, Y. (2016). Inorganic elemental determinations of marine traditional Chinese Medicine Meretricis concha from Jiaozhou Bay: The construction of inorganic elemental fingerprint based on chemometric analysis. *Journal of Ocean University of China, 15*, 357–362. https://doi.org/10.1007/s11802-016-2749-7

24 Hu, Y., Wang, Y., Deng, J., & Jiang, H. (2015). The structure of a prophenoloxidase (PPO) from Anopheles gambiae provides new insights into the mechanism of PPO activation. *BMC Biology, 14*(2), 1–13. https://doi.org/10.1186/s12915-015-0225-2

25 He, T.Z., Yuan, J.D., LI, W., He, B., & Duan, H.G. (2015). Enzymatic Properties of Polyphenol Oxidase from Dysosma versipellis (Hance.) M. Cheng. *Food Sci., 36*(13), 137–142. https://doi.org/10.7506/spkx1002-6630-201513026

26 Li, D. (2017). Studies on the Interaction of Cefepime Hydrochloride with Bovine Serum Albumin by Fluorescence, Synchronous Fluorescence, Three-Dimensional Fluorescence and Circular Dichroism. *Journal of Bioanalysis & Biomedicine*, 1–7. https://doi.org/10.4172/1948-593X.1000162

27 Magdum, P.A. Gokavi, N.M., & Nandibewoor, S.T. (2017). Study on the interaction between anti-tuberculosis drug ethambutol and bovine serum albumin: multispectroscopic and cyclic voltammetric approaches. *Lumin., 32*(2), 206–216. https://doi.org/10.1002/bio.3169

28 Gu, Y., Wang, Y., & Zhang, H. (2018). Study on the interactions between toxic nitroanilines and lysozyme by spectroscopic approaches and molecular modeling. *Spectrochim. Acta, Part A, 202*, 260–268. https://doi.org/10.1016/j.saa.2018.05.008

29 Li, J.H., Bian, L., Tian, S.Y., Kong, J.M., & Zhu, L.Z. (2017). Spectroscopic study on the interaction of human cytoglobin with copper (II) ion. *Spectrosc. Spectral Anal., 37*, 321–326. https://doi.org/10.3964/j.issn.1000-0593(2017)01-0321-06

30 Fernández-Sainz, J., Pacheco-Liñán, P.J., & Granadino-Roldán, J.M. (2017). Binding of the anticancer drug BI-2536 to human serum albumin. A spectroscopic and theoretical study. *J. Photochem. Photobiol. B, Biology, 172*, 77–87. https://doi.org/10.1016/j.jphotobiol.2017.05.016

31 Jiang, Y.Y., Wang, X.L., Wang, H.H., Zhang, L., Wang, H., Ji, L.N., & Liu, H.Y. (2016). The Interaction Between a New Water-Soluble Meso-Tetrakis (Carboxyl) Zinc (–) Porphyrin and Human Serum Albumin. *Spectrosc. Spectral Anal., 36*(9), 2894–2900. PMID: 30084622

32 An, X., Zhao, J., Cui, F., & Qu, G. (2017). The investigation of interaction between Thioguanine and human serum albumin by fluorescence and modeling. *Arabian Journal of Chemistry, 10*, 2935–2947. https://doi.org/10.1016/j.arabjc.2013.06.031

33 García-Jiménez, A., Teruel-Puche, J.A., Berna, J.L., Rodríguez-López, J.N., Tudela, J., García-Ruíz, P.A., & García-Cánovas, F. (2016). Characterization of the action of tyrosinase on resorcinols. *Bioorganic & medicinal chemistry, 24*(18), 4434–4443. https://doi.org/ 10.1016/j.bmc.2016.07.048

34 Ploch-Jankowska, A., & Pentak, D. (2020). A Comprehensive Spectroscopic Analysis of the Ibuprofen Binding with Human Serum Albumin, Part I. *Pharmaceuticals, 13*, 205–230. https://doi.org/10.3390/ph13090205

35 Wani, T.A., Bakheit, A.H., Zargar, S., Rizwana, H., & Al-majed, A. (2019). Evaluation of competitive binding interaction of neratinib and tamoxifen to serum albumin in multidrug therapy. *Spectrochimica acta. Part A, Molecular and biomolecular spectroscopy, 117691*(19), 31081-9. https://doi.org/10.1016/j.saa.2019.117691

Цуйюнь Ву, Ваньцин Лин, Есен Яо, Мин Гуо, Нуршат Нурадже

Полифенол оксидазасын кумар қышқылымен байланыстырудың биополимерлік жүйесінің үш өлшемді саусақ іздері спектроскопия әдісімен зерттеу

Табиғаттағы биохимиялық процестерде антиоксидант болып келетін кумар қышқылын (КҚ) қорғау үлкен қызығушылық тудыруда. Полифенолоксидазасы (ПФО) көкөністер, жемістер мен саңырау-құлақтар сияқты өсімдіктердің ескіруі мен қараюында маңызды рөл атқаратын фермент болып табылады. КҚ және ПФО өзара әрекеттесуі метаболизм мен ескіру туралы маңызды ақпарат береді. Сондықтан, КҚ-ын полифенолоксидазасымен (ПФО) байланыстырудың молекулалық механизмі спектроскопиялық әдістерді молекулалық модельдеумен біріктіру арқылы зерттелді. Алғаш рет КҚ мен ПФО арасындағы биополимердің өзара әрекеттесуін сипаттау үшін КҚ-ПФО кешенінің үш өлшемді іздері жасалды. Спектроскопиялық әдістерді қолдану КҚ ПФО өзіндік флуоресценциясын тиімді түрде басатындығын көрсетті. Энтальпияның өзгеруі ($\Delta H°$) және энтропияның өзгеруі ($\Delta S°$) КҚ-ПФО кешені негізінен КҚ және ПФО гидрофобты әрекеттесуімен тұрақтандырылған деп болжайды. КҚ-ПФО кешенінің λ-UV-F ізінің құрылысы КҚ мен ПФО арасындағы үш өлшемді өзара әрекеттесуді көрсетуге мүмкіндік берді. Кейіннен молекулалық модельдеу КҚ мен ПФО негізінен гидрофобты өзара әрекеттесулер мен Ala202, His38, His54 және Ser206 аминқышқылдарының қалдықтарында орналасқан сутегі байланыстарымен байланысты екенін көрсетті. Компьютерлік модельдеу КҚ-ПФО өзара әрекеттесуі үшін анықталған үш өлшемді модельге деген сенімділікті көрсететін спектрлік эксперименттерге сәйкес келді.

Кілт сөздер: биополимер, құрамында Cu бар фермент, кумар қышқылы, полифенол оксидазы, антиоксидант, α-пирон-5-карбон қышқылы, спектроскопия, тирозиназа, молекулалық модельдеу.

Цуйюнь Ву, Ваньцин Лин, Есен Яо, Мин Гуо, Нуршат Нурадже

Исследование методом трехмерной спектроскопии отпечатков пальцев биополимерной системы связывания полифенолоксидазы с кумаровой кислотой

Защита кумаровой кислоты (КК), антиоксиданта, в биохимическом процессе в природе вызвала большой интерес. Полифенолоксидаза (ПФО) — это фермент, который играет жизненно важную роль в старении и потемнении растений, таких как овощи, фрукты и грибы. Взаимодействие КК и ПФО раскрывает важную информацию о метаболизме и старении. Поэтому молекулярный механизм связывания КК с полифенолоксидазой (ПФО) был исследован путем объединения спектроскопических методов с молекулярным моделированием. Впервые был создан трехмерный отпечаток комплекса КК–ПФО для характеристики взаимодействия биополимера между КК и ПФО. Применение спектроскопических методов показало, что КК эффективно подавляет собственную флуоресценцию ПФО. Изменение энтальпии ($\Delta H°$) и энтропии ($\Delta S°$) предполагает, что комплекс КК–ПФО был преимущественно стабилизирован гидрофобными взаимодействиями КК и ПФО. Построение λ-UV-F отпечатка КК–ПФО позволило продемонстрировать трехмерные взаимодействия между КК и ПФО. Впоследствии молекулярное моделирование показало, что КК, в основном, связана с ПФО гидрофобными взаимодействиями и водородными связями, расположенными в аминокислотных остатках Ala202, His38, His54 и Ser206. Компьютерное моделирование соответствовало спектральным экспериментам, демонстрирующим уверенность в трехмерной модели, определенной для взаимодействия КК–ПФО.

Ключевые слова: биополимер, Cu-содержащий фермент, кумаровая кислота, полифенолоксидаза, антиоксидант, α-пирон-5-карбоновая кислота, спектроскопия, тирозиназа, молекулярное моделирование.

Information about authors[*]

Wu, Cuiyun — Candidate of Chemical Sciences, Leading Researcher of Red jujube fruit team, Tarim University, A'ler, 843301, Xinjinag, China; e-mail: wcyby@163.com; https://orcid.org/0000-0002-0178-3524;

Ling, Wanqing — Master of chemical sciences, assistant researcher, Zhejiang Agriculture and Forestry University, 310007, Lin'an City, Hangzhou, Zhejiang, China; e-mail: lwq9901@163.com;

Yao, Yecen — Master of Chemical Sciences, Assistant Researcher, Zhejiang Agriculture and Forestry University, 310007, Lin'an City, Hangzhou, Zhejiang, China; e-mail: 2020104062016@zafu.edu.cn;

Guo, Ming — PhD in Chemistry, Professor at Zhejiang Agriculture and Forestry University, 310007, Lin'an City, Hangzhou, Zhejiang, China; e-mail: guoming@zafu.edu.cn; https://orcid.org/0000-0002-5255-9952;

Nuraje, Nurxat — PhD in Chemistry, Head of ASEMS, National Laboratory Astana, Nazarbayev University, Kabanbay batyr avenue, 53, 010000, Nur-Sultan, Kazakhstan; e-mail: nurxat.nuraje@nu.edu.kz; https://orcid.org/0000-0003-4751-2719

*The author's name is presented in the order: *Last Name, First and Middle Names*